Dynamic modelling and energy performance analysis of an innovative dual-source heat pump system

DYNAMIC MODELLING AND ENERGY PERFORMANCE ANALYSIS OF AN INNOVATIVE DUAL-SOURCE HEAT PUMP SYSTEM

Ilaria Grossi [a], Matteo Dongellini [a*], Gian Luca Morini [b]

[a] *Centro Interdipartimentale di Ricerca Industriale Edilizia e Costruzioni, Alma Mater Studiorum – Università di Bologna, Via del Lazzaretto 15/5, Bologna, 40131, Italy*, ilaria.grossi@studio.unibo.it, matteo.dongellini@unibo.it

[b] *Department of Industrial Engineering, School of Engineering and Architecture, Alma Mater Studiorum – Università di Bologna, Viale Risorgimento 2, Bologna, 40136, Italy, gianluca.morini3@unibo.it*

[*] *corresponding author*

ABSTRACT

In this paper the energy performance of a dual-source heat pump (*DSHP*) system able to use both air and ground as external heat source is analysed by using *TRNSYS17*. The *DSHP* seasonal and annual performance factors are compared with those offered by the same *DSHP* in which only ground (ground-source mode) or only external air (air-source mode) is used as external heat source in order to evaluate the benefits achievable with the exploitation of a double external heat source (ground and air) with the same unit. Yearly dynamic simulations have been carried out by coupling the *DSHP* to a detached residential building located in Bologna, characterized by unbalanced heating and cooling loads, and coupled to a geothermal loop based on borehole heat exchangers (*BHEs*). With the help of the dynamic simulations it has been demonstrated that *DSHPs* can be very useful in order to solve the problems linked to the ground temperature drift which can be originated by the presence of an undersized borehole heat exchanger field and/or by unbalanced heating and cooling loads. In fact, the use of external air as auxiliary heat source with respect to ground during the winter enables to obtain more stable energy performance even in presence of undersized *BHE*s. In this paper it is shown how an optimal trade-off in terms of annual energy performances and investment costs can be obtained by reducing the size of the *DSHP* borehole field of 15-55% with respect to the borehole field needed by a

conventional ground-coupled heat pump having the same size. In this way the *DSHP* can be used during the retrofitting of thermal plants based on ground-coupled heat pumps in which an undersized *BHE* field is present.

Keywords: dual-source heat pumps, ground-coupled heat pumps, air-source heat pumps, dynamic simulations, unbalanced building loads.

LIST OF SYMBOLS

APF	Annual performance factor defined by Eq.(1) [-]
D	Diameter of borehole [m]
d_{ext}	External diameter of U-tube [m]
d_{int}	Internal diameter of U-tube [m]
H	Half distance between the centre of the borehole and the centre of U-tube [m]
L_0	Borehole maximum length [m]
P	Fan-coil thermal power [W]
*PBT**	Normalized Payback time defined by Eq.(2) [-]
Q	Heat delivered to the building [kWh]
R_b	Thermal resistance of borehole mortar [m^2KW^{-1}]
RH	Relative humidity [%]
R_{pe}	Thermal resistance of the U-tube [m^2KW^{-1}]
SCOP	Seasonal coefficient of performance defined by Eq.(1) [-]
SEER	Seasonal energy efficiency ratio defined by Eq.(1) [-]
t	Time [hr]
T	Temperature [°C]
$T_{b,in}$	Brine temperature at the inlet of the heat pump [°C]
$T_{w,in}$	Water temperature at the inlet of fan-coils [°C]
U-value	Trasmittance value [$Wm^{-2}K^{-1}$]

U_{lim}	Trasmittance limit value [$Wm^{-2}K^{-1}$]
V	Volumetric flow rate [lh^{-1}]
W	Electrical energy input [kWh]

Greek symbols

α	Thermal diffusivity [m^2s^{-1}]
ΔC	Over-cost [€]
ΔT_{fc}	Water temperature difference between the fan-coil inlet and outlet [K]
ΔT_g	Annual ground temperature drift [K]
λ	Thermal conductivity [$Wm^{-1}K^{-1}$]
Π_p	Pump electric power [W]

Subscripts

air	Internal air
c	Cooling value
des	Design value
ext	Outdoor value
g	Ground value
h	Heating value
i	*i*-th hour
in	Inlet value
ins,f	Insulation of floor
ins,r	Insulation of roof
min	Minimum value
switch	Switch value
opt	Optimal value
w	Water

1. INTRODUCTION

During the last years, European Community focused its attention on the exploitation of renewable energy sources with the aim to reduce the primary energy demand of many anthropogenic activities such as public transports, industrial and agricultural sectors, heating and cooling of buildings. Heat pumps are indicated in a series of recent EU Directive *[1-3]*, among other systems, as strategic devices for the next generation of heating and cooling systems due to their capacity to exploit a significant amount of renewable energy from natural thermal sources, like aerothermal, geothermal and hydrothermal sources.

This framework has enhanced the diffusion of heat pumps in Europe especially during the last five years. The EHPA 2015 statistics report *[4]* shows how the heat pump market in Europe from 2005 to 2014 increased of about 50%. In 2014, the European market was mainly made up of air-source heat pumps and ground-coupled heat pumps, able to cover 70% and 10% respectively of the whole European market with a further increase of 20% of the number of air-source heat pump sold from 2014 to 2015.

As demonstrated by many authors, heating systems based on air-source heat pumps can reduce the primary energy consumptions linked to heating and cooling of buildings if compared to traditional systems based on gas boilers and chillers *[5-7]*. However, due to the significant variation of the external air temperature during the year, these systems are characterized by variable energy performances which tend to decrease during the coldest (in heating mode) and hottest (in cooling mode) periods. In addition, the energy performance of air-source heat pumps is reduced also in presence of mild external air temperature values in humid climates, during the winter season, due to the significant defrosting energy losses *[8-9]*. In order to defrost the external heat exchanger, air-source heat pumps perform periodically a series of defrosting cycles which have a twofold penalization effect: they determine an energy cost for the heating system coupled to a reduction of the temperature of the hot water produced, which can cause an indoor discomfort in the building.

The use of external heat sources more stable in terms of temperature both during winter and summer can significantly enhance the heat pump efficiency as demonstrated by many authors who compared the energy performance of air-source heat pumps with those of heat pumps which use ground *[10]*, grey-water *[11]* and surface water *[12]* as external heat sources. Among the above-mentioned cases, ground-coupled heat pumps have demonstrated excellent values of seasonal energy performance factors, both for heating and cooling of

buildings, thanks to the thermal stability of the ground *[13]*. However, the diffusion of these systems has been, up to now, limited by the high investment costs linked to the need of a geothermal loop based on a Borehole Heat Exchanger (BHE) field. During the design of a heating and cooling system based on a ground-coupled heat pump, a crucial aspect that must be carefully considered by the designer is the correct sizing of the boreholes field *[14-15]*. In fact, in presence of undersized *BHEs* and/or unbalanced heating and cooling thermal loads the ground temperature tends to decrease (in cold areas) or increase (in hot areas) year by year; this behaviour can penalize the heat pump during its operative life by decreasing its annual energy performance. In order to take into account this aspect, it becomes mandatory to conduct a long-term performance analysis of the boreholes field in order to verify if the ground temperature drift year by year can be considered acceptable for a stable behaviour of the system both in heating and cooling. In many cases, an incorrect sizing of the borehole field, responsible of a progressive reduction of the energy efficiency of the heating and cooling system, has conducted to a replacement of the system after few years from its start-up *[16]*.

To overcome the limits of both air-source (low efficiency) and ground-coupled (high costs) heat pumps, in this paper an innovative double source heat pump (*DSHP*) able to use alternatively two external heat sources, air and ground, is presented. In literature a series of dual-source systems have been already proposed; in many cases, these systems are obtained by coupling a conventional heat pump (i.e. *GCHP*) with an additional system which can be a heat compensator *[16]*, a cooling tower *[17]* or a solar collector *[18-19]*. The dual-source heat pump presented in this paper is different; in this case the heat pump has two external heat exchangers which can be used alternatively in order to exploit heat from ground or air. From a theoretical point of view, this kind of heat pump allows to obtain higher energy performances with respect to the conventional air-source heat pumps, thanks to the use of ground during the coldest winter hours, and it is characterized by lower costs compared to a conventional ground-coupled heat pump, thanks to the reduced size of the BHEs field which needs to be coupled to the heat pump.

In a *DSHP* the switch between air and ground heat sources can be decided in different ways: i) by maximizing the instantaneous energy performance of the system; ii) by maximizing the annual performance of the system; iii) by minimizing the energy costs. In the first case the switch is driven by the instantaneous value of

the external source temperature (air or ground), while in the second case the switch is decided by taking into account the design heating and cooling building loads together with the penalties linked to the ground temperature variation and the defrost cycles. In the third case the availability of self-produced electric energy (i.e. by means of PV systems) must be taken into account in order to decide which external source has to be used hour by hour.

Up to now, a systematic analysis of the energy performance of *DSHP* units coupled to a building as a function of the size of the BHE and of the switch rules between air and ground is missing. For this reason, in this paper the analysis of the yearly energy performances of a *DSHP* coupled to a residential building is presented by modelling the whole system (i.e. *DSHP*, distribution loop, terminal units and building) with *TRNSYS17 [20]*. The evaluation of the main energy performance indicators is obtained by varying the size of the borehole field coupled to the *DSHP* with the aim to verify if an optimal reduction of the borehole length there exists when air is used as secondary external heat source in a typical climate of North Italy. The seasonal and annual energy performance of the *DSHP* system have been evaluated and compared with those achievable by using the *DSHP* as an air-source heat pump (air-source mode) or as a ground-coupled heat pump (ground-source mode) with the aim to explore in which operative conditions a *DSHP* can be competitive with the conventional monovalent systems based on heat pumps.

2. THE CASE STUDY

In order to assess the energy performances of a *DSHP* for heating and cooling, a single-family residential building located in Bologna (Northern Italy, 44°29’37” N) has been selected; in this application the heat pump allows to maintain the indoor set-point temperature equal to 20°C and 26°C during heating and cooling season, respectively. The heat pump is the only generator of the heating and cooling system, avoiding the use of back-up systems.

2.1 Building data

The building is a one-storey single-family house built ten years ago with a net floor area equal to 70 m^2 and composed by four rooms; in Figure 1 the floor plan of the building is shown.

The flat is characterized by a net conditioning volume equal to 300 m^3 and a surface to volume ratio *S/V* equal to 0.37 m^{-1}. A summary of the main geometrical characteristics of each room (net floor area, external surface area, windows area) is reported in Table 1.

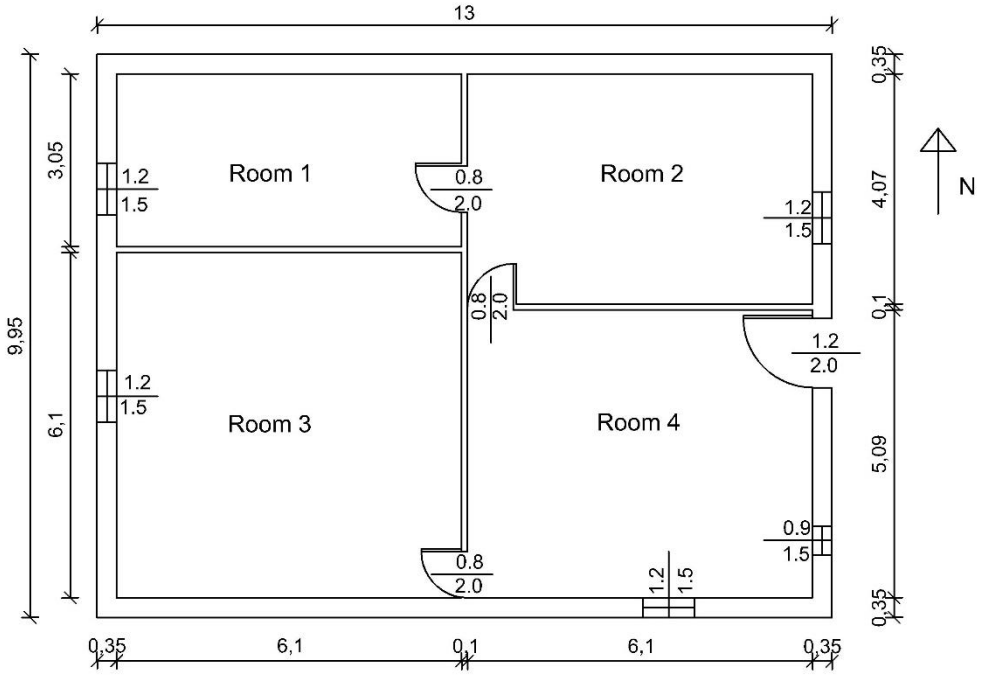

Figure 1: Floor plan of the one-storey house.

Table 1: Geometrical characteristic of the thermal zones.

Zone	Net floor area [m^2]	External surface area [m^2]	Windows area [m^2]	Net volume [m^3]
Room 1	18.6	29.9	1.8	50.2
Room 2	24.8	32.9	1.8	67.0
Room 3	37.2	39.0	1.8	100.5
Room 4	31.0	36.0	3.2	83.8
Attic	113.9	107.2	0	269.1
Total	225.5	245.0	8.6	570.6

The opaque elements of the building envelope are characterized by a good insulation level: the main thermal characteristics of these elements, as well as the windows properties are summarized in Table 2. The *U*-values linked to the main envelope elements highlight that their level of thermal insulation is good even if not optimal; in fact, in some case the *U*-values of the envelope components are larger than the maximum values of the actual Italian transmittance limits, U_{lim}, reported in Table 2 as well.

The external walls and the slab on grade floor are insulated with 6 cm of thermal insulation ($\lambda_{ins,f}$= 0.040 $Wm^{-1}K^{-1}$), while in the roof 8 cm of polystyrene ($\lambda_{ins,r}$ = 0.038 $Wm^{-1}K^{-1}$) are inserted. Transparent elements consist of a low-emissivity double glass (4/12/4) filled with Argon, with an emissivity value of 0.1 (glass transmittance equal to 1.5 $Wm^{-2}K^{-1}$); the frame covers 20% of the total window area and its transmittance is equal to 1.77 $Wm^{-2}K^{-1}$.

Table 2: U-values of the main building envelope components.

Envelope component	*U*-value [$Wm^{-2}K^{-1}$]	U_{lim} [$Wm^{-2}K^{-1}$]
External wall	0.38	0.30
Internal wall	1.79	0.80
Floor	0.31	0.30
Roof	0.22	0.25
Ceiling	1.01	0.30
Window	1.77	1.80

Thanks to *TRNSYS17* the heating and cooling loads of the building have been calculated and are reported in Figure 2 as a function of the external air temperature, following the building energy signature method [21]. The climatic data of the Test Reference Year (*TRY*) defined by METEONORM [22] for Bologna have been used for the dynamic simulation. Following the *TRY* of Bologna, the minimum external air temperature during winter is -7°C (heating season design temperature, $T_{des,h}$); this value has been considered as design temperature for the heat pump sizing during heating operating mode. The maximum external air temperature during summer is 35°C (cooling season design temperature, $T_{des,c}$). In Figure 2 the heating load of the building (red line) is shown as a function of the external air temperature. In correspondence of the external design temperature (-7°C) the maximum heating load required by the building is equal to 8.6 kW. The building cooling loads have been calculated following the same procedure and the summer building energy signature has been represented in Figure 2 (blue line). It is evident that cooling loads are lower than heating loads (unbalanced loads); more in detail, comparing winter and summer building energy signatures it is evident that the heating design load (8.6 kW) is about 3 times larger than the cooling design load (2.8 kW).

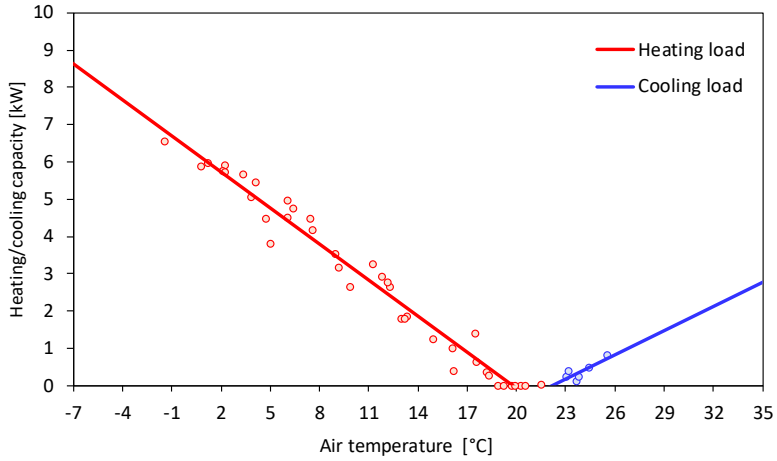

Figure 2: Building heating and cooling loads as a function of the external air temperature.

2.2 HVAC system modeling

The HVAC system is based on an invertible heat pump coupled to four two-pipe fan-coils, one for each room, by means of a two-pipes hydronic loop (single loop). In Table 3 the technical data of the selected 3-speed fan-coils are shown.

Table 3: Technical data of the 3-speed fan-coils.

	Room 1 and 3 (V_w=315 lh^{-1})			Room 2 (V_w=256 lh^{-1})			Room 4 (V_w=408 lh^{-1})		
Fan speed	V_{air} [m^{3}h^{-1}]	P_c [1][W]	P_h [2][W]	V_{air} [m^{3}h^{-1}]	P_c [1][W]	P_h [2][W]	V_{air} [m^{3}h^{-1}]	P_c [1][W]	P_h [2][W]
Min	211	1740	1530	178	1380	1240	241	2260	1780
Med	271	2010	1810	233	1540	1470	341	2720	2350
Max	344	2180	2100	319	1730	1770	442	3030	2830

[1] cooling conditions: $T_{w,in}$ =7°C, ΔT_{fc} = -5 K, T_{air}=26°C RH=60%

[2] heating conditions: $T_{w,in}$ = 45°C, ΔT_{fc} = 5 K, T_{air}=20°C

In the hydronic loop is present an inertial water tank (120 litres) able to increase the thermal inertia of the distribution loop with the aim to reduce the number of the on-off cycles performed by the heat pump during the milder part of the heating season and during summer, when the heat pump is called to work under a reduced load, and to stabilize the water temperature at the fan-coil inlet during the heat pump defrost cycles. An innovative inverter-driven Dual-Source Heat Pump (*DSHP*) has been considered as heat generator coupled to the building. The heat pump is designed in order to cover the maximum heating and cooling load of the building without back-up systems (monovalent system). The *DSHP* is able to operate by using as external heat source, alternatively, air or ground.

2.2.1 Borehole heat exchangers

In order to use ground as external source the *DSHP* is coupled to a geothermal loop obtained by means of a series of vertical double U-type borehole heat exchangers (*BHE*s), see Figure 3, where brine (mixture of water and propylene glycol at 25%, density of 1038 kgm^{-3}, specific heat of 3.714 $kJkg^{-1}K^{-1}$) is used as working fluid. The vertical boreholes have a diameter (*D*) of 152 mm; they are composed by a double U-tube made in polyethylene characterized by a thermal resistance (R_{pe}) of 0.355 m^2KW^{-1}, in which the gap between the U-tube and the ground is filled with sealant mortar (thermal resistance (R_b) of 1.6 m^2KW^{-1}). The U-tube external diameter (d_{ext}) is 32 mm and the internal diameter (d_{int}) is 26 mm. The half distance between the centre of the borehole and the centre of U-tube (*H*) is 83 mm (see Figure 3).

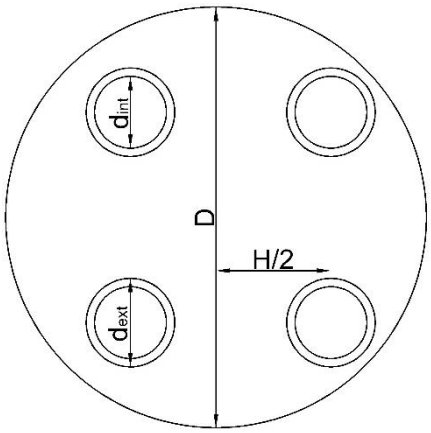

Figure 3: Geometry of the vertical double U-type boreholes.

In order to evaluate the *BHE* sizing, the thermal characteristics of the soil must be taken into account. In literature values of the thermal power exchanged between the boreholes and the ground range from 30 Wm^{-1} [23] to 50 Wm^{-1} [24]. In this case study, the ground is considered composed of one clay, silt and gravel layer, with a thermal conductivity (λ_g) of 1.97 $Wm^{-1}K^{-1}$ and a thermal diffusivity (α_g) of 8.28 E-07 m^2s^{-1}, characterized by a thermal power exchanged equal to 40 Wm^{-1}. By using this value, it is possible to evaluate that 2 vertical double U-type boreholes, each 105 m long and placed at a distance of 6 m one from the other, are able to match the maximum building heating load.

2.2.2 The Dual-Source Heat Pump

In Figure 4 the layout of the *DSHP* prototype is shown; the logical scheme of the heat pump is similar to the typical layout of a reversible multi-function heat pump with condensation-heat recovery for domestic hot water production during the summer [25]. In fact, in a multi-function heat pump there are two external heat exchangers which are used, during the summer season, alternatively to discharge heat to the external air or to produce domestic hot water thanks to the condensation heat recovery. The same architecture can be used in order to obtain a *DSHP* able to switch during the whole year from air to ground thanks to two external heat exchangers: a fin-and-tube heat exchanger for the air-source mode and a plate heat exchanger for the ground-coupled mode.

The *DSHP* prototype can work as an inverter-driven air-to-water heat pump (air-source mode) or as an inverter driven brine-to-water heat pump by switching from an external heat exchanger to the other. When the plate heat exchanger is used, the heat pump can be connected to a BHEs field in order to use ground as external source (ground-source mode). This prototype has been developed in the frame of the HEGOS project, funded by the European Community, by modifying a commercial reversible multi-function heat pump with condensation-heat recovery for domestic hot water production (Galletti model HWMC010).

Experimental tests on the dynamic behaviour of the *DSHP* prototype are currently running in the climatic room of the Laboratory of Applied Thermal Engineering of University of Bologna by following the hardware-in-the-loop approach [26].

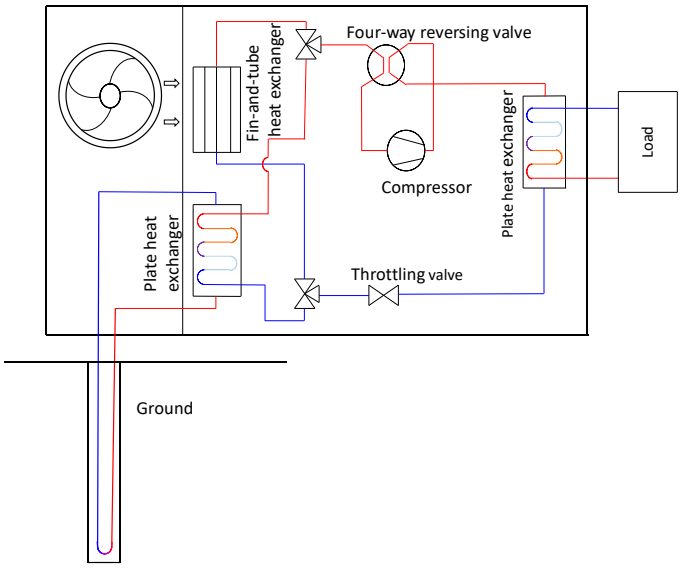

Figure 4: Layout of the DSHP prototype.

A series of experimental tests have been conducted in order to obtain the characteristic curves of this new heat pump. The *DSHP* performance data, evaluated when the unit operates by using air as external source (air-source mode), are reported in Figure 5, while the characteristic curves obtained by using the external plate heat exchanger (ground-source mode) are shown in Figure 6.

The curves reported in Figure 5 and 6 have been obtained by considering the water temperature delivered by the heat pump ($T_{w,in}$) equal to 45°C for the heating mode and 7°C for the cooling mode. The inverter frequency was varied during tests from 30 Hz to 110 Hz (i.e. the whole frequency range). In Figure 5a the heating capacity and *COP* of the *DSHP* under air-source mode is shown as a function of the external air temperature for three values of frequency (30 Hz, 70 Hz, 110 Hz). In Figure 5b the cooling capacity and *EER* of the *DSHP* under air-source mode is reported as a function of the external air temperature for the same values of frequency considered in Figure 5a.

By comparing Figure 5 with Figure 2 it is evident that the *DSHP* under air-source mode is able to cover the maximum heating load (8.6 kW at -7°C) of the building; on the contrary, the *DSHP* is strongly oversized during summer with respect to the building maximum cooling load (5.4 kW vs 2.8 kW at 35°C).

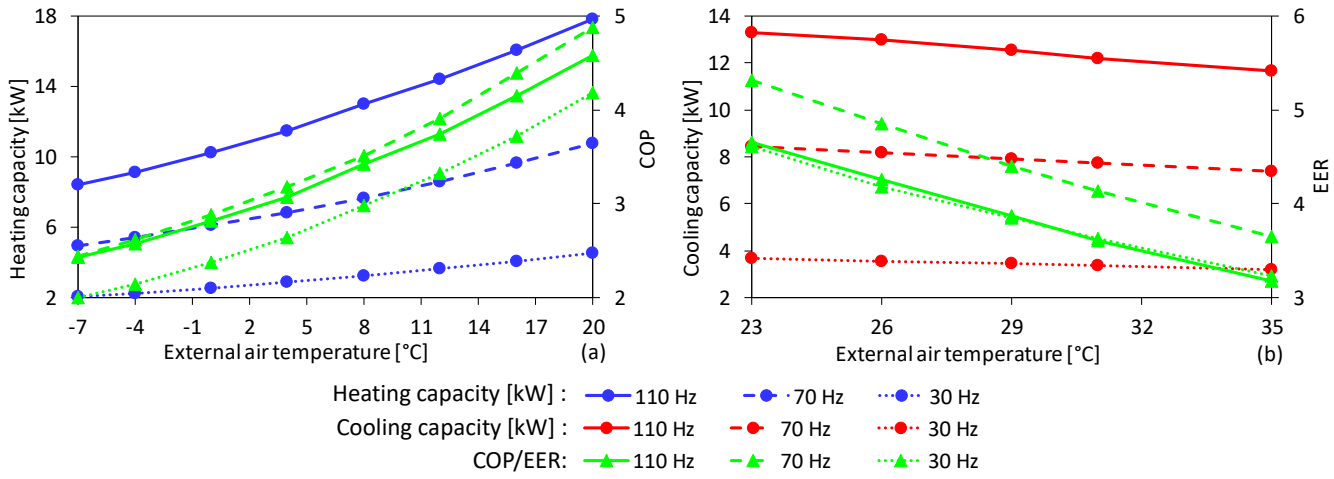

Figure 5: (a) Heating capacity and COP (b) Cooling capacity and EER of the DSHP (air-source mode) as a function of the external air temperature for three values of frequency (30 Hz, 70 Hz, 110 Hz).

In Figure 6 the characteristic curves of the *DSHP* operating in ground-source mode are reported as a function of the brine temperature at the inlet of the heat pump ($T_{b,in}$) and of the inverter frequency. The heating

capacity and *COP* are reported in Figure 6a and the cooling capacity and *EER* are reported in Figure 6b, respectively.

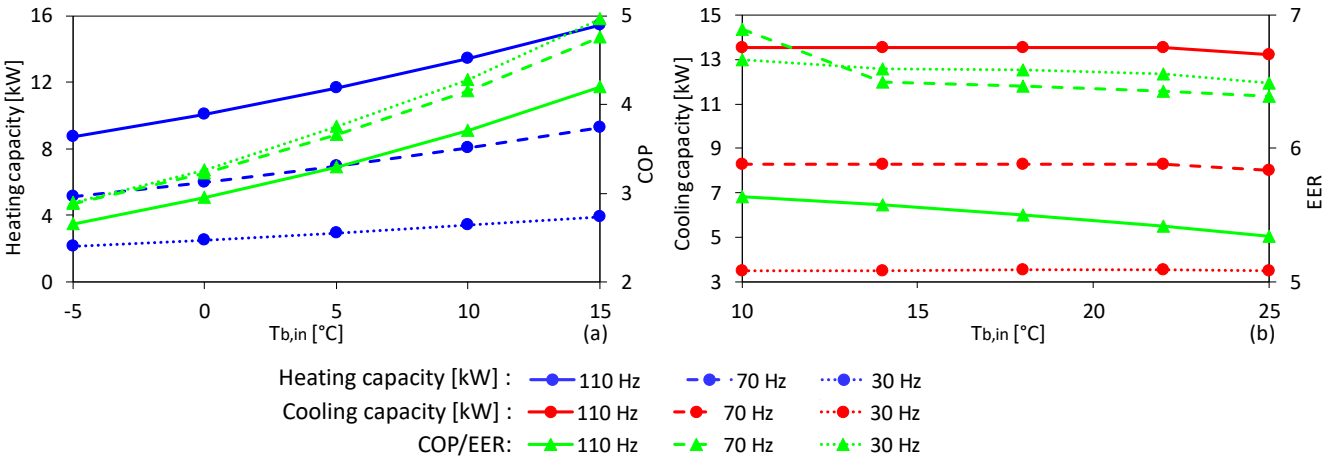

Figure 6: (a) Heating capacity and COP (b) Cooling capacity and EER of the DSHP (ground-source mode) as a function of the brine temperature at the inlet of the heat pump for three values of frequency (30 Hz, 70 Hz, 110 Hz).

Operating with the external plate heat exchanger the *DSHP* prototype is able to cover the maximum heating load of the building (11.7 kW at 5°C of brine at the inlet of the plate heat exchanger) and it is strongly oversized in summer (13.5 kW vs 2.8 kW, see Section 2.1).

By comparing Figure 5 and Figure 6 it is evident that when the *DSHP* operates by using the external air heat exchanger (air-source mode) the heat pump energy performance strongly depends on the value assumed by the external air temperature (T_{ext}). On the contrary, when the *DSHP* operates by using the external plate heat exchanger with brine (ground-source mode) the cooling and heating performances are weakly dependent on the external air temperature, since the heat pump energy performance are only influenced by the ground temperature (T_g) which depends on the size of BHEs field coupled to the heat pump.

2.2.3 Heat pump control

The DSHP is an inverter driven unit able to modulate the delivered thermal power by modifying the compressor rotating speed according to the inverter effective frequency. The heat pump control strategy is based on a PI controller which uses the supply water temperature $T_{w,out}$ as monitoring variable. The set-point value of the supply water temperature has been set in heating mode to 45°C and to 7°C in cooling mode.

When the inverter operates at the minimum frequency no further modulation of the delivered thermal power is possible; in this case, an on-off control logic characterized by a hysteresis cycle is followed by the heat pump. The on-off control strategy is based on a dead band of 5 K centred on the set-point value (45°C in winter and 7°C in summer). The on-off logic maintains the inverter at the minimum frequency until the supply water temperature is higher than 47.5°C (in winter) or lower than 4.5°C (in summer); when these limit values are overcame, the heat pump is switched off. Then, the heat pump is switched on when the supply water temperature decreases below 42.5°C (in winter) or above 9.5°C (in summer). In Figure 7 the hysteresis cycles of the on-off control logic followed by the *DSHP* when the inverter minimum frequency is reached are shown both for winter (Figure 7a) and summer (Figure 7b).

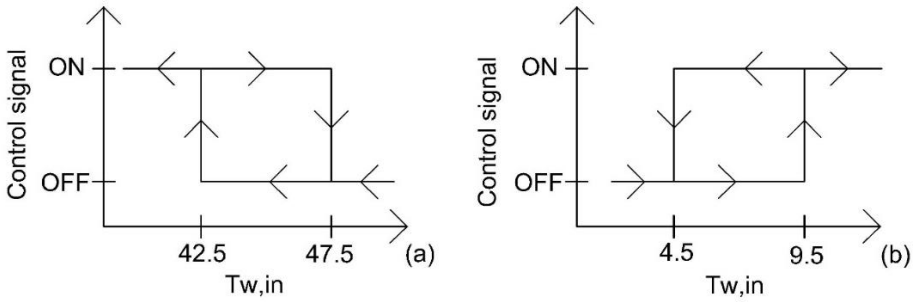

Figure 7: Hysteresis cycles of the DSHP on-off controller at the minimum inverter frequency; (a) heating season, (b) cooling season.

In addition to the conventional control rules described before, the *DSHP* needs specific control rules in order to select the external heat exchanger called to work. Different rules can be followed to switch from air-source to ground-source. In this paper the switch between the air heat exchanger and the brine heat exchanger is decided on the basis of the value assumed by the external air temperature. When the external air temperature is lower than the switch temperature (T_{switch}), a fixed value of temperature which can be selected by the designer, the *DSHP* changes its operating mode from air to ground-source mode. On the contrary, when the external air temperature is larger than the switch temperature (T_{switch}) the *DSHP* switches from ground to air-source mode. In the next Sections, thanks to a series of numerical simulations, the value of T_{switch} which maximizes the annual energy performance of the whole system is determined.

3. DYNAMIC SIMULATION

The seasonal and annual energy performance of the *HVAC* system described in the previous Section have been evaluated by using the dynamic simulation software *TRNSYS17*. The dynamic model of the inverter driven *DSHP* has been obtained by customizing the standard Types for heat pumps included in the *TRNSYS* library by introducing the specific characteristic curves of the *DSHP* shown previously (Figure 5 and 6). In Figure 8 the *TRNSYS17* model of the whole system is shown. The model is composed by: (i) the building; (ii) the hydronic loop which connects the heat generator to the terminal units (i.e. fan-coils); (iii) the air-source side of the *DSHP*, in which the most important elements are the PID controller for the heat pump inverter and the lookup table containing the values of heating power, *COP*, cooling power and *EER* derived by the experimental tests for different heat pump operating conditions; (iv) the ground-source side of the *DSHP*, similar to the previous one but with the addition of the standard *TRNSYS* Type which simulates the behaviour of the *BHE*s. In this Type the physical properties of the ground and of the fluid flowing within the heat exchangers (i.e. brine), the number, the length and the distance among the boreholes are introduced.

The *TRNSYS* model shown in Figure 8 can be used in order to model two sub-cases in which the *DSHP* is forced to operate as a conventional heat pump by using only one of the two external heat exchangers. In this way the *DSHP* is transformed in a conventional inverter driven air-source heat pump (air-source mode) or in a classical inverter-driven ground-coupled heat pump (ground-source mode).

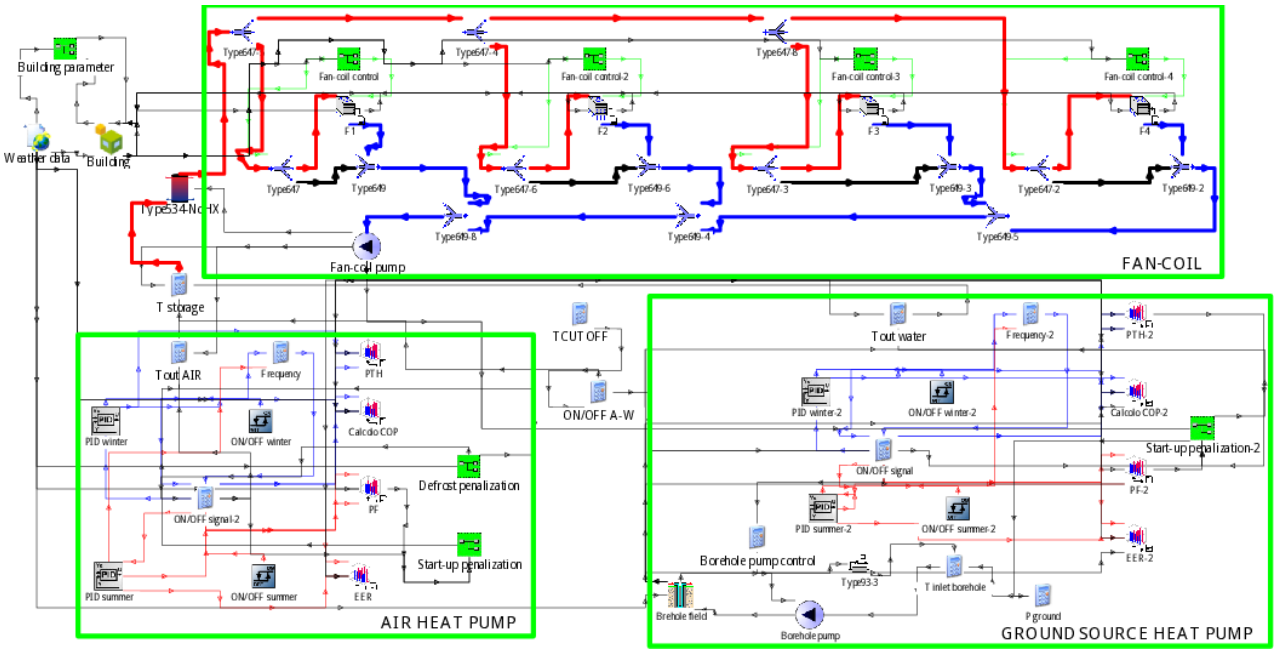

Figure 8: TRNSYS layout of the HVAC system based on DSHP.

The main key performance indicators used to compute the seasonal and the annual energy performance of the system are the Seasonal Coefficient of Performance (*SCOP*) for the heating season, the Seasonal Energy Efficiency Ratio (*SEER*) for the cooling season and the Annual Performance Factor (*APF*), a global parameter able to represent the annual energy performance of the system. The definition of these parameters is the following:

$$\begin{cases} SCOP = \frac{\sum_{i=0}^{t_{heating}} Q_{h,i}}{\sum_{i=0}^{t_{heating}} W_i} \\ SEER = \frac{\sum_{i=0}^{t_{cooling}} Q_{c,i}}{\sum_{i=0}^{t_{cooling}} W_i} \\ APF = \frac{\sum_{i=0}^{8760\ h} (Q_{h,i}+Q_{c,i})}{\sum_{i=0}^{8760\ h} W_i} \end{cases} \quad (1)$$

where S*COP* is defined as the ratio between the thermal energy delivered by the heat pump during the winter season (t_h) and the total electric energy consumption of the heat pump during the same period: $Q_{h,i}$ represents the thermal energy delivered to the building during the *i*-th hour by the heat pump and W_i stands for the total electric energy consumption of the heat pump during the same hour. Similarly, *SEER* is obtained as the ratio between the cooling energy delivered by the heat pump and the total electric energy consumption of the heat pump during the summer season. $Q_{c,i}$ and W_i represent the cooling energy supplied by the heat pump and the electrical energy input during the *i*-th hour, respectively. Finally, *APF* is defined as the ratio between the thermal/cooling energy delivered by the heat pump during both winter and summer season and the total electric energy consumption of the heat pump during the whole year. In presence of the *BHEs* field the electric energy demand of the geothermal loop circulating pumps (electrical power input Π_p equal to 33 W) is taken into account for the seasonal and annual performance factors calculation.

3.1 Validation of the TRNSYS model for BHEs field long-term evaluation

Before to start with the numerical simulation of the three heat pump configurations described before, a verification of the long-term results obtained by using the standard *TRNSYS* type for the *BHE*s modeling have been made by comparing the *TRNSYS* results with those obtained by using a *MATLAB* code based on the *g-function method* [15], following the procedure proposed by Naldi et al. [27]. The *g-function method* is considered the most accurate method to obtain a good prediction of the time evolution of the mean

temperature at the interface between the borehole and the ground for a single borehole heat exchanger. The effects of other boreholes are evaluated by employing the superposition of effects in space. The values of the brine temperature incoming to the heat pump from the boreholes field ($T_{b,in}$) and the heat pump performance over 15 years, obtained by means of the *TRNSYS* models, have been compared with those obtained by using a *MATLAB* script based on the procedure described in [27].

Different cases have been considered in this validation process by considering the borehole field composed by: 1) 2 boreholes 105 m long (L_0), 2) 2 boreholes 75 m long (0.7 L_0) and 3) 1 borehole 105 m long (0.5 L_0).

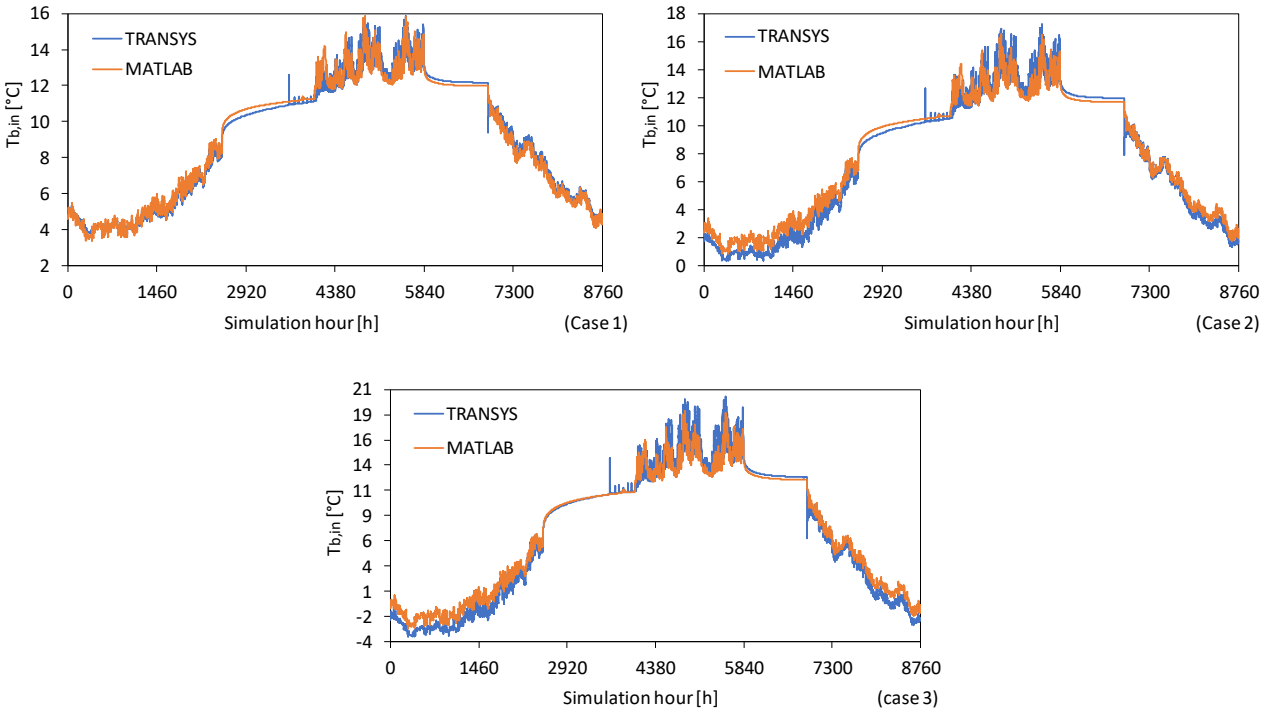

Figure 9: Comparison between the brine temperature at the heat pump inlet ($T_{b,in}$) obtained by using TRNSYS and MATLAB [27] during the 7th year of simulation: (case 1) BHE field having a total length of L_0 (=2x105m) (case 2) BHE field having a total length of 0.7 L_0 (=2x75m) (case 3) BHE field having a total length of 0.5 L_0 (=1x105m).

In Figure 9 the comparison between the values of inlet brine temperature at the heat pump during the 7th year of simulation obtained by using *TRNSYS* and the *MATLAB* script based on the *g-functions* is shown for the three cases considered. It is possible to see that the results obtained with *TRNSYS* are in good agreement with those obtained with the most accurate method based on the *g-functions*.

The average difference between the brine temperature at the outlet of the borehole field obtained with *TRNSYS* and *MATLAB* for the case of a total length of the *BHE*s equal to L_0 (=2 x105 m, Figure 9 Case 1) is less

than 0.3°C; in the case of a length of the *BHE*s equal to 0.7 L_0 (=2 x 75 m, Figure 9 Case2) the average difference is less than 0.5°C and for a length of 0.5 L_0 (=1x105 m, Figure 9 Case3) the difference is lower than 0.8°C.

In order to evaluate the impact of these variations in terms of brine temperature on the main energy performance indicators introduced by Eq.(1) in Table 4, 5 and 6 the values of *SCOP*, *SEER* and *APF* obtained by considering the *DSHP* operating in ground-source mode during the whole year are shown.

The values of *SCOP, SEER* and *APF* reported in Table 4, 5 and 6 are obtained by ignoring the start-up penalization and the energy consumption of the auxiliary pumps of the geothermal loop because the *MATLAB* script based on the procedure described in [27] does not take into account these parameters.

Table 4: Comparison of seasonal and annual performance for a BHEs field having a total length equal to L_0 (=2x105m)

Year of simulation	*SCOP*			*SEER*			*APF*		
	TRNSYS	*MATLAB*	Difference [%]	*TRNSYS*	*MATLAB*	Difference [%]	*TRNSYS*	*MATLAB*	Difference [%]
1st year	3.73	3.96	-6.0	5.24	5.59	-6.7	3.81	4.04	-6.0
5th year	3.63	3.84	-5.8	5.24	5.59	-6.7	3.72	3.93	-5.9
15th year	3.61	3.81	-5.5	5.24	5.59	-6.7	3.70	3.90	-5.6

Table 5: Comparison of seasonal and annual performance for a BHEs field having a total length equal to 0.7 L_0 (=2x75m)

Year of simulation	*SCOP*			*SEER*			*APF*		
	TRNSYS	*MATLAB*	Difference [%]	*TRNSYS*	*MATLAB*	Difference [%]	*TRNSYS*	*MATLAB*	Difference [%]
1st year	3.49	3.70	-6.2	5.24	5.59	-6.7	3.58	3.80	-6.3
5th year	3.38	3.58	-6.0	5.24	5.59	-6.7	3.47	3.68	-6.1
15th year	3.36	3.55	-5.7	5.24	5.59	-6.7	3.45	3.65	-5.7

Table 6: Comparison of seasonal and annual performance for a BHEs field having a total length equal to 0.5 L_0 (=1x105m)

Year of simulation	*SCOP*			*SEER*			*APF*		
	TRNSYS	*MATLAB*	Difference [%]	*TRNSYS*	*MATLAB*	Difference [%]	*TRNSYS*	*MATLAB*	Difference [%]
1st year	3.20	3.43	-7.2	5.25	5.60	-6.7	3.29	3.53	-7.2
5th year	3.12	3.34	-6.9	5.24	5.60	-6.7	3.22	3.44	-6.9
15th year	3.11	3.32	-6.6	5.24	5.60	-6.7	3.21	3.42	-6.6

For all cases the values of the energy performance indicators obtained by means of the *MATLAB* script are larger than those obtained with *TRNSYS*; the maximum difference between the two approaches is less than 7.2%. It is possible to conclude that the results obtained with *TRNSYS* are in a very good agreement with those obtained by using a more accurate method for the long-term analysis of the behaviour of the *BHEs* field. As a consequence, the *TRNSYS* model of the vertical *BHEs* field can be used in order to study the short and long-term effects of the variation of the borehole length on the energy performance of the *DSHP*.

4. DISCUSSION OF THE RESULTS

In this Section the main numerical results obtained by means of the *TRNSYS* dynamic simulations are shown and discussed in detail. Three case studies are considered: (i) *HVAC* system based on a *DSHP* operating in air-source mode (Case A); (ii) *HVAC* system based on a *DSHP* operating in ground-source mode (Case B); (iii) *HVAC* system based on a *DSHP* (Case C). In this way the results of the dynamic simulations can be used in order to understand in which conditions a *DSHP* can be a suitable alternative to the conventional air- or ground-source heat pumps. More in detail, yearly and long-term (over 15 years) simulations have been carried out for each case analysed.

In Case A (air-source mode) the simulations have been carried out by considering the *DSHP* operating only with the external fin-and-tube heat exchanger during the whole year. In this way the *DSHP* works like a traditional inverter-driven air-to-water heat pump. The calculation takes into account both on-off cycling losses [28] and defrost cycles penalization [29]. The start-up-time penalty degradation effect has been implemented directly in the *TRNSYS* model by using a series of experimental values obtained during the dynamic tests on the *DSHP* prototype. More in detail, based on these experimental observations, the model considers during the start-up phase the *COP* of the heat pump reduced of 28-31% with respect to its nominal value for the first 216 seconds when the heat pump is switched on.

In addition, defrost penalization effect is taken into account in the dynamic model of the heat pump. The calculation of the defrost energy losses is based on the simplified model proposed by Vocale at al. [9]; during the initial stand-by period of a defrost cycle (30 seconds), the reversing valve of the heat pump is activated and the fan of the outdoor coil is stopped. After this period, the heat pump operates following the cooling

cycle. On the basis of the experimental measures made on the *DSHP*, when the heat pump operates in reverse mode the thermal power supplied to the outdoor heat exchanger is equal to 11.4 kW and the unit works with an *EER* equal to 6. A typical defrost cycle runs for 360 seconds; after this period, the frost thermostat opens the circuit, then the defrost cycle stops, the four-way valve reverses and the unit returns to the heating cycle after a second stand-by period equal to 30 seconds.

In Case B (ground-source mode) the simulations have been carried out by considering the *DSHP* operating only with the external plate heat exchanger during the whole year. In this way the *DSHP* works like a traditional inverter-driven brine-to-water heat pump. In this case the calculation takes into account on-off cycles penalization as well.

Finally, in Case C (*DSHP* mode) the *DSHP* is able to switch between the two external heat exchangers during the year on the basis of the external air temperature. On-off cycles penalization and defrost energy losses have been taken into account in the calculation of the seasonal and annual energy performance of the *DSHP*.

4.1 Case A: air-source mode

Inhibiting the use of the external plate heat exchanger of the *DSHP*, the building heating/cooling loads are fulfilled by a traditional inverter-driven air-source heat pump without any back-up heater. In this case, the energy performance of the system is strongly influenced by the modulating capacity of the device and by the defrosting cycles activated during the winter season.

In Figure 10 the monthly trend of the thermal energy supplied to the building during the heating (blue columns) and cooling (orange columns) season and the cooling energy (yellow columns) subtracted to the system during the defrost cycles are shown.

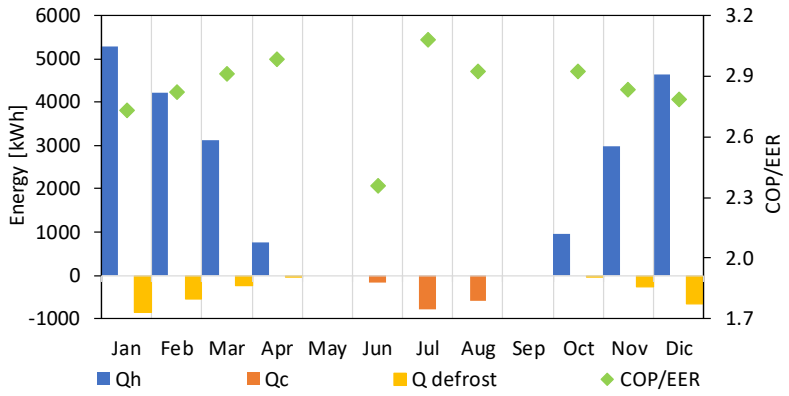

Figure 10: Monthly heating/cooling energy supplied to the building (Q_{th}, Q_c), thermal energy supplied during defrost cycles ($Q_{defrost}$) and COP/EER obtained in air-source mode.

With the typical climate of Bologna characterized by a mild temperature in winter coupled to high humidity ratio values, the heat pump has to perform 2060 defrost cycles in a year; the electric energy consumption of the unit during this operating mode accounts to about the 6% of the whole electric energy input of the winter season. In addition, thanks to the inverter and to the inertial tank, the average number of heat pump on-off cycles is equal to 2 on-off cycles per hour in winter, below the maximum value of 6 cycles per hour suggested by the compressor manufacturers. Since the heat pump is strongly oversized in summer, the number of on-off cycles performed by the unit during the cooling season justifies the low values of *EER* highlighted in Figure 10. In June, the *EER* value of 2.3 is caused by the large electric energy consumption due to the circulating pumps of the hydronic loops compared to the cooling energy delivered by the heat pump.

The system works with a *SCOP* value of 2.79 during the winter season and with a *SEER* of 2.92 during the cooling season. The *APF* of the system is around 2.80; values of *APF* lower than 3 are typical for air-source heat pumps systems coupled to buildings located in the Northern Italy with unbalanced loads (heating loads larger than cooling loads), as demonstrated in [6].

4.2 Case B: ground-source mode

Inhibiting the use of the external air heat exchanger of the *DSHP*, the building heating/cooling loads are fulfilled by a traditional inverter-driven brine-to-water heat pump coupled to a geothermal loop without any back-up heater. In this case the seasonal and annual performance of the system are strongly influenced by the sizing of the boreholes field. As described in Section 2.2.1, 2 boreholes 105 m long are able to match the

maximum building heating load. With the aim to take into account the influence of the building unbalanced thermal loads between winter and summer on the ground temperature drift, a long-term dynamic simulation (15 years) have been performed. In Table 7 the values of the energy performance indicators obtained in correspondence of the first and of the fifteenth year are shown.

Table 7: Variation of the main energy performance indicators from the first to the fifteenth year by considering the DSHP working in ground-source mode.

SCOP			*SEER*			*APF*		
1st	15th	[%]	1st	15th	[%]	1st	15th	[%]
3.52	3.42	-2.8	4.25	4.25	0	3.57	3.47	-2.8

By observing the data reported in Table 7 it is evident that the energy efficiency of the heat pump slightly decreases during the first fifteen years of work. This small variation is linked to the low thermal drift of the ground temperature due to the unbalanced building loads (see Figure 2). In fact, even in presence of a building with unbalanced load, during the first year the difference of the ground temperature between the beginning of the winter period and the end of the cooling period (ΔT_g) is lower than 0.5 K. In order to give an idea of the decrease of the ground temperature year by year, the average ground temperature is equal to 13.2°C during the first year of operation and after 15 years decreases to 9.7°C (ΔT_g<3.5 K in fifteen years). This progressive cooling of the ground causes a small reduction of *APF* (-2.8% after 15 years), as highlighted by data reported in Table 7. This result confirms that the sizing of the *BHEs* field is correct.

By comparing the values of *SCOP, SEER* and *APF* obtained with *DSHP* in ground-source mode with those obtained by using air as external thermal source, an increase of 24% in terms of *SCOP*, 45% in terms of *SEER* and 25% in terms of *APF* can be observed. This increase is mainly due to the stability of the ground temperature during the whole year with respect to the external air temperature.

4.3 Case C: DSHP mode

In this case the heat pump can switch between the two external heat exchangers; the heat pump is able to exploit heat from the external air as well as the ground thanks to a geothermal loop based on a *BHEs* field. A simple control strategy based on a fixed value of the switching temperature (T_{switch}) is adopted in order to

switch between air and ground sources: if the external air temperature is lower than T_{switch} the *DSHP* works by using the plate heat exchanger coupled to the geothermal loop (ground-source mode); on the contrary, when the external air temperature is larger than T_{switch} the *DSHP* works by using the external air as heat source (air-source mode).

Five different configurations of the borehole field have been considered, as summarized in Table 8; each case is characterized by a different length of the borehole heat exchangers. In Case C1 the *BHEs* field is the same of Case B.

Table 8: Configurations of the BHEs field coupled to DSHP.

	Case C1	Case C2	Case C3	Case C4	Case C5
Borehole configuration (number x length)	2 x 105 m	2 x 90 m	2 x 75 m	1 x 105 m	1 x 90 m
Total length	L_0	0.86 L_0	0.71 L_0	0.50 L_0	0.43 L_0

In Figure 11a the *APF* values obtained by using the *DSHP* as generator for building space heating and cooling are shown in correspondence of the 7th year of simulation as a function of the adopted switching temperature.

Considering a *BHEs* field of total length equal to L_0 (case C1) the *APF* maximum value is obtained for large switching temperature values; in this case the heat pump uses mainly the external plate heat exchanger and the geothermal loop and the *APF* value tends to the value obtained in Case B. As an example, adopting a switching temperature equal to 14°C the *DSHP* exploits ground source during 88% of the year and about 94% of the building heating energy demand is covered by using ground source. On the contrary, adopting a low value of the switching temperature the heat pump maximizes the use of external air as heat source and the energy performances of the system tend to those obtained in Case A. In this latter case the size of the *BHEs* field does not influence the *APF* value.

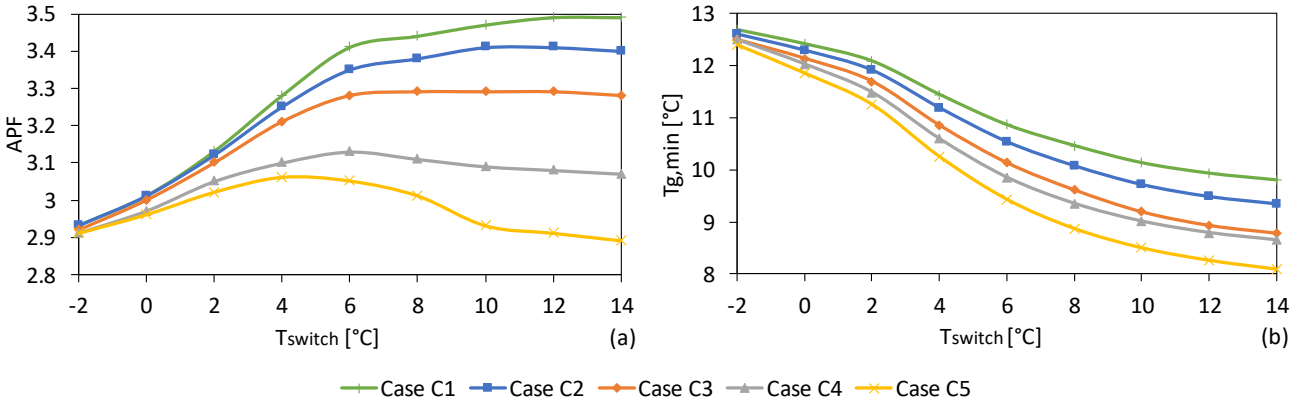

Figure 11: (a) APF *and (b) yearly minimum ground temperature as a function of the switching temperature for cases C1, C2, C3, C4, C5 in correspondence of the 7th year of simulation.*

The capability to use two external sources allows to reduce the dimension of the boreholes field with respect to cases B and C1 (total length of *BHEs* field equal to L_0) and to decrease the plant investment costs. If the total length of the field is reduced the *APF* value decreases and an optimal value of the switching temperature, in correspondence of which *APF* is maximum, can be determined. This means that it is possible to obtain an optimal switching temperature for each borehole field coupled to the *DSHP*.

In Figure 11b the trend of the yearly minimum value of the ground temperature ($T_{g,min}$) obtained for each case by varying the switching temperature of the *DSHP* is shown. The minimum ground temperature decreases if the size of the borehole field is reduced and, for a fixed total length of the vertical boreholes, $T_{g,min}$ decreases if the switching temperature is increased.

In Table 9 the energy performance indicators obtained at 7th year of simulation and the optimal switching temperature ($T_{switch,opt}$) are shown as a function of the borehole field size. In addition, the values of the ground temperature drift (ΔT_g) after 15 years of simulation are also reported.

Table 9: Optimal switching temperature ($T_{switch,opt}$), ground temperature drift (ΔT_g) after 15 years, seasonal and annual energy performance indicators as a function of the BHE field size.

Case	$T_{switch,opt}$ [°C]	ΔT_g [K]	*SCOP*	*SEER*	*APF*
C1 (L_0)	14	3.4	3.44	4.30	3.49
C2 (0.86 L_0)	10	3.5	3.35	4.30	3.41
C3 (0.71 L_0)	8	3.7	3.23	4.31	3.29
C4 (0.50 L_0)	6	3.7	3.07	4.32	3.13
C5 (0.43 L_0)	4	4.6	2.99	4.32	3.06

The values reported in Table 9 highlight that the optimal switching temperature is larger than 6°C, except for Case C5 in which the borehole field is strongly undersized. Adopting a switching temperature larger than 6°C no defrost cycles are needed; as a consequence, both comfort (no inversion of the cycle for defrosting cycles) and economical (reduced dimensions of the borehole field) benefits can be obtained. Furthermore, in Table 9 the difference between the maximum (reached at the beginning of the simulation) and the minimum (reached at the end of simulation) ground temperature is shown as a function of the borehole field sizing.

The results shown in Table 9 underline how the adoption of a *DSHP* is able to mitigate the negative effect of the building unbalanced loads by damping the oscillation of the ground temperature also with undersized borehole field. In fact, the use of air as auxiliary external heat source helps the soil to restore its temperature even in presence of unbalanced loads. This result demonstrates that a correct sizing of *DSHP* systems allows to eliminate the undesired ground thermal drift in presence of building unbalanced loads and to reduce the size of the *BHE* field. For this reason, *DSHP* can be proposed for the retrofitting of thermal plants based on ground-coupled heat pumps in which an undersized *BHE* field is present.

4.4 Comparisons

In Table 10 a comparison among the cases presented before in terms of use of the external heat sources (air and ground) is shown. For case C1, C2, C3, C4, C5 the optimal switching temperature reported in Table 9 has been considered. If the switching temperature is increased, the size of the *BHE* field must be increased because the *DSHP* mainly uses ground as external source. On the contrary, a reduction of the *BHEs* size determines a lower optimal switching temperature and an increase of the use of the air source. In addition, in Table 10 the percentage of the building energy demand for space heating covered by exploiting air or ground sources is also shown. During the summer season in each case the *DSHP* works only by using the ground source to restore the ground temperature since the thermal and cooling request of the building are strongly unbalanced.

Table 10: Use of the external heat sources (air and ground) during the winter season.

Case	Air-source mode operating time [%]	Ground-source mode operating time [%]	Building energy demand covered by air source [%]	Building energy demand covered by ground source [%]
B	0	100	0	100
C1	6.9	93.1	5.8	94.2
C2	21.8	78.2	19.3	80.7
C3	34.0	66.0	27.4	72.6
C4	47.7	52.3	40.0	60.0
C5	47.7	52.3	40.0	60.0
A	100	0	100	0

In

Table 11 a comparison among the main energy performance indicators obtained for the analysed cases is shown. Only Cases C2, C3, C4 and C5 are retained because Case C1 gives similar results to Case B. Case A is taken as baseline in order to evaluate the variation of the energy performance indexes.

The results show that *DSHP* is able to guarantee better annual energy performances with respect to the air-source heat pump (from +9% to +25%) but lower to those of a ground-source heat pump (from -2% to -14%). However, the use of two external sources allows to the *DSHP* to guarantee a more stable *SCOP* and *APF* during the fifteen years of operation with respect to Case B. Furthermore, the worsening of the energy performance indicators going from Case B to Cases C2, C3, C4 is coupled to the decrease of the investment costs due to the adoption of shorter borehole fields. The results of Table 11 suggest that with a *DSHP* it becomes possible to reduce the length of the *BHEs* field up to 50% in presence of building unbalanced loads, ensuring *APF* values larger of 10-20% with respect to a conventional air-source heat pump and installation costs lower of 16-30% with respect to a conventional ground-coupled heat pump.

Table 11: Comparison among the energy performance indicators obtained for the studied cases.

		SCOP		*SEER*		*APF*	
		1st year	15th year	1st year	15th year	1st year	15th year
Ground-source mode	(Case B)	3.52	3.42	4.25	4.25	3.57 (+27.5%)	3.47 (+24.0%)
	(Case C2)	3.40	3.35	4.31	4.31	3.49 (+24.6%)	3.41 (+21.8%)
DSHP	(Case C3)	3.27	3.22	4.31	4.31	3.33 (+18.9%)	3.28 (+17.1%)
	(Case C4)	3.09	3.07	4.32	4.32	3.15 (+12.5%)	3.13 (+11.8%)

	(Case C5)	3.00	2.99	4.32	4.32	3.07 (+9.6%)	3.06 (+9.3%)
Air-source mode	(Case A)	2.79	2.79	2.92	2.92	2.80	2.80

In Figure 12 the *APF* values for Cases A, B, C2, C3, C4 and C5 are reported togheter with the typical investment costs of the adopted systems by taking into account the installation costs of both heat pump unit and borehole field. The cheaper heat pump is the air-source heat pump (Case A); on the contrary, the most expensive unit is the *DSHP* due to the presence of two external heat exchangers. In Figure 12 the borehole field cost (i.e. 50 €m^{-1}) is evidenced with the aim to put in evidence that in some case this cost becomes predominant (i.e. Case B). With the adoption of a *DSHP*, the investment due to the borehole field installation decreases and the total cost of the *DSHP* systems (Cases C2, C3 and C4) is lower than that of Case B but higher than that of Case A.

By observing Figure 12, if a *DSHP* is adopted, the investment cost is reduced with respect to a ground-source heat pump (Case B) of a percentage variable from 6% (Case C2) to 32% (Case C5).

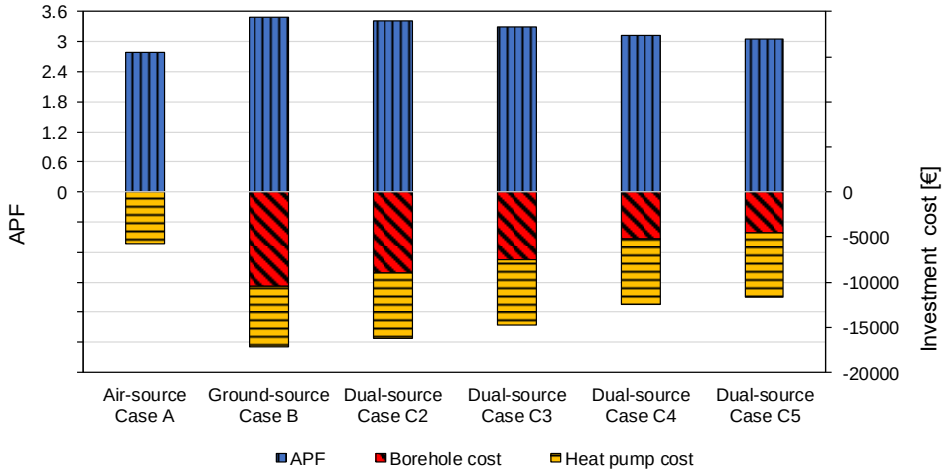

Figure 12 : Comparison between APF and investment costs for Cases A, B, C2, C3, C4 and C5.

It is possible to calculate the Payback time (*PBT*) of the different solutions with respect to the cheaper solution (air-source heat pump). The Payback time is defined as the length of time required to recover the cost of the investment thanks to the energy saving obtained. A normalized Payback time (*PBT**) is obtained by scaling the calculated Payback time on the Payback time originated by the replacement of an air-source heat pump (Case A) with a ground-source heat pump (Case B):

$$PBT^{*}_{I-A} = \frac{\Delta C_{I-A}}{\Delta C_{B-A}} \frac{\left(\frac{1}{APF_A} - \frac{1}{APF_B}\right)}{\left(\frac{1}{APF_A} - \frac{1}{APF_I}\right)} \quad I = \{B, C1, C2, C3, C4\} \tag{2}$$

where ΔC_{I-A} is the over-cost of the generic Case I with respect to Case A (air-source heat pump), ΔC_{B-A} is the over-cost of Case B (ground-source heat pump) with respect to Case A. The normalized *PBT** defined by Eq. (2) is not dependent on the unitary cost of the supply energy (electric energy in this case) but it depends on the annual energy performance of the system (*APF*) and on the over-costs with respect to the cheaper solution (Case A).

In Figure 13 the normalized Payback time *PBT** is shown by considering for each solution the investment costs indicated in Figure 12. A value of *PBT** lower than 1 means a shorter Payback time with respect to the case in which the air-source heat pump is replaced by the ground-coupled heat pump.

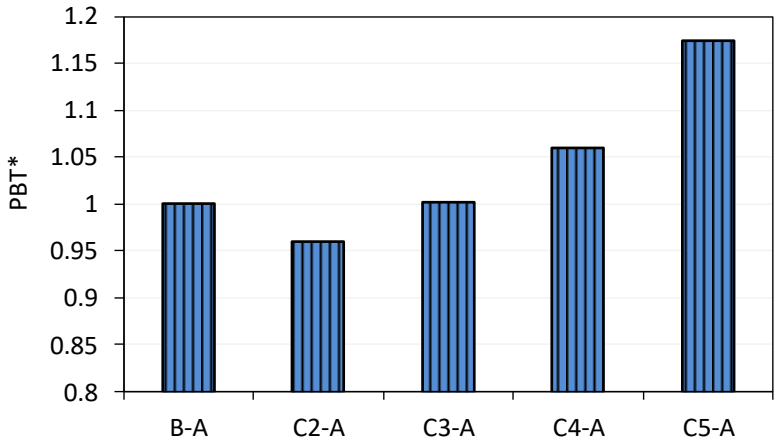

Figure 13: Normalized Pay Back Time by taking as baseline the system based on the air-source heat pump (Case A).

It is possible to appreciate that with a reduction of the *BHEs* field of 30% (Case C3) the normalized Payback time is around 1. With a reduction of the BHE field up to 50% a normalized Payback time equal to 1.05 is obtained. This result confirms that a reduction of the *BHE* field of the order of 30-50% with respect to Case B, in terms of Payback time is equivalent to replace an air-source heat pump with a ground-coupled heat pump with the advantage to reduce the ground temperature drift and to stabilize the energy performance indicators even in presence of buildings with strongly unbalanced loads.

A reduction of the borehole heat exchanger costs can increase significantly the value of the *PBT** if a *DSHP* is adopted and this solution becomes less attractive.

5. CONCLUSIONS

In this paper an analysis of the seasonal and annual energy performances of an innovative dual-source heat pump (*DSHP*) able to use as external heat source both ground and outdoor air is presented.

The *DSHP* prototype is derived by a commercial reversible multi-function heat pump with condensation-heat recovery for domestic hot water production during the summer season. The heat pump is designed in order to be able to use alternatively two external heat exchangers by working in air-source mode (thanks to an external fin-and-tube heat exchanger) or in ground-coupled mode (using a plate heat exchanger). By using the experimental characteristic curves of the *DSHP* prototype, a dynamic model of the unit is made by means of *TRNSYS17*, by taking into account the energy losses linked to the activation of defrost cycles and to the on-off penalization. A series of numerical simulations have been presented by coupling the *DSHP* prototype to a one-storey single-family house sited in Bologna (Northern Italy) characterized by unbalanced heating and cooling loads (heating loads much larger than the cooling ones). This situation is usually dangerous for a stable behaviour of a ground coupled heat pump because the ground temperature can evidence a significant drift year by year due to the incapability of the ground to recover the temperature level during the summer season. In order to study the capability of a *DSHP* to reduce the ground temperature drift in presence of buildings with unbalanced loads, the long-term interaction between the borehole heat exchanger and the ground has been modelled in *TRNSYS* and the results have been validated by using the *g-function method.* The dynamic simulations, extended to 15 years, have been used in order to determine the optimal value of the switching temperature which allows to the *DSHP* prototype to select the external heat exchanger during the winter season on the basis of the value assumed by the external air temperature. It has been demonstrated that the optimal switching temperature depends on the size of the borehole heat exchanger field coupled to the *DSHP*. In general, a lower switching temperature is needed in presence of shorter boreholes in order to maximize the annual energy performance factor of the *DSHP*. It has been demonstrated that the adoption of a *DSHP* can strongly reduce the ground temperature drift, stabilizing the heat pump performance during the years. In addition, a reduction of the *BHEs* length coupled to the heat pump of the order of 30-50% with respect to the borehole field needed by a conventional ground coupled heat pump can guarantee stable and high energy performance factors of the system in presence of strongly unbalanced

loads: in fact, in this case the energy losses linked to the defrost cycles are avoided and the investment costs are strongly reduced. The results shown in this paper demonstrate that the *DSHP* prototype can be a good option for all the cases in which the long-term ground temperature drift, due to the presence of unbalanced loads and/or an incorrect sizing of the *BHE* field, is significant. Additional work is needed in order to optimize the *DSHP* performances as well as to introduce innovative switch rules between air and ground (i.e. in presence of free electric energy produced during the day by using renewable energy). In summary, a *DSHP* can be suggested for the replacement of conventional ground-coupled heat pumps in presence of undersized *BHEs*.

6. ACKNOWLEDGMENTS

The research has received funding in the frame of the European Regional Development Fund POR-FESR 2014-2020 Programme (Regional funds of Emilia Romagna) under grant agreement n° CUP D92I16000050009.

7. REFERENCES

[1] E.U. Directive 2009/28/EC on the Promotion of the use of energy from renewable sources, 23 April 2009.

[2] E.U. Directive 2010/31/EU of the European Parliament and of the Council of on the Energy Performance of Buildings, 19 May 2010.

[3] E.U. Directive 2012/27/EU on Energy Efficiency, amending Directives 2009/12/EC and 2010/30/EU and repealing Directives 2004/8/EC and 2006/32/EC, 25 October 2012.

[4] EHPA European Heat Pump Market and Statistics Report 2015: executive summary 2015, http://www.ehpa.org/market-data/2015/.

[5] M. Dongellini, C. Naldi, G.L. Morini, Seasonal performance evaluation of electric air-to-water heat pump systems, Applied Thermal Engineering 90 (2015) 1072-1081.

[6] V. Bianco, F. Scarpa, L.A. Tagliafico, Estimation of primary energy savings by using heat pumps for heagting purposes in the residential sector, Applied Thermal Engineering 114 (2017) 938-947.

[7] M. Dongellini, C. Naldi, G.L. Morini, Sizing effects on the energy performance of reversible air-source heat pumps for office buildings, Applied Thermal Engineering 114 (2017) 1073-1081.

[8] F. Wang, C. Liang, X. Zhang, Research of anti-frosting technology in refrigeration and air conditioning fields: A review, Renewable and Sustainable Energy Reviews 81 (2018) 707-722.

[9] P. Vocale, G.L. Morini, M. Spiga, Influence of outdoor air conditions on the air source heat pumps performance, Energy Procedia 45 (2014) 653-662.

[10] J.F. Urchueguía, M. Zacarès, J.M. Corberàn, Á. Montero, J. Martos, H. Witte, Comparison between the energy performance of a ground coupled water to water heat pump system and an air to water heat pump system for heating and cooling in typical conditions of the European Mediterranean coast, Energy Conversion and Management 49 (2008) 2917-2923.

[11] X. Liu, S.-K. Lau, H. Li, Optimization and analysis of a multi-functional heat pump system with air source and gray water source in heating mode, Energy and Buildings 69 (2014) 1-13.

[12] S. Kindaichi, D. Nishina, L. Wen, T. Kannaka, Potential for using water reservoirs as heat sources in heat pump systems, Applied Thermal Engineering 76 (2015) 47-53.

[13] S.J. Self, B.V. Reddy, M.A. Rosen, Geothermal heat pump systems: Status review and comparison with other heating options, Applied Energy 101 (2013) 341-348.

[14] S.H. Park, J.Y. Kim, Y.S. Jang, E.J. Kim, Development of a multi-objective sizing method for borehole heat exchangers during the early design phase, Sustainability 9 (2017) 1876.

[15] S. Lazzari, A. Priarone, E. Zanchini, Long-term performance of BHE (borehole heat exchanger) fields with negligible groundwater movement, Energy 35 (2010) 4966-4974.

[16] T. You, W. Shi, B. Wang, W. Wu, W. Li, X. Li, A new ground-coupled heat pump system integrated with a multi-mode air-source heat compensator to eliminate thermal imbalance in cold regions, Energy and Buildings 107 (2015) 103-112.

[17] R. Fan, Y. Gao, Y. Pan and Y. Zhang, Research on cool injection and extraction performance of borehole cool energy storage for ground coupled heat pump system, Energy and Buildings 101 (2015) 35-44.

[18] R. Chargui ,S. Awani, Determining of the optimal design of a closed loop solar dual source heat pump system coupled with a residential building application, Energy Conversion and Management 147, (2017) 40-54.

[19] R.M. Lazzarin, Dual source heat pump systems: Operation and performance, Energy and Buildings 52 (2012) 77-85.

[20] S.A. Klein, W.A. Beckman, J.W. Mitchell, J.A. Duffie, N.A. Duffie, T.L. Freeman., TRNSYS: A Transient System Simulation Program., Solar Energy Laboratory, University of Wisconsin, Madison USA (2010).

[21] M. F. Fels, PRISM: An Introduction, Energy and Buildings 9 (1986) 5-18.

[22] METEONORM, Global Meteorological Database for Solar Energy and Applied Climatology, Version 5, (http://www.meteotest.com).

[23] C.K. Lee, H.N. Lam, Computer simulation of borehole ground heat exchangers for geothermal heat pump systems, Renewable Energy 33 (2008) 1286-1296.

[24] G. Florides, K. Soteris, Ground heat exchangers - A review of systems, models and application, Renewable Energy 32 (2007) 2461-2478.

[25] C. Naldi, E. Zanchini, Dynamic simulation during summer of a reversible multi-function heat pump with condensation-heat recovery, Applied Thermal Engineering 116 (2017) 126–133.

[26] A. Piazzi, I. Grossi, M. Magni, M. Dongellini, J.P. Campana, G.L. Morini, The “Hardware-in-the-loop” approach for the experimental test of an innovative dual-source heat pump, in Proceedings of 16th International Conference on Sustainable Energy Technology (SET2017), Bologna, Italy, 2017.

[27] C. Naldi, E. Zanchini, Effects of the total borehole length and of the heat pump inverter on the performance of a ground-coupled heat pump system, Applied Thermal Engineering 128 (2018) 306-319.

[28] M. Dongellini, M. Abbenante, G.L. Morini, A strategy for the optimal control logic of heat pump systems: impact on the energy consumptions of a residential building, in Proceedings of 12th IEA Heat Pump Conference 2017, Rotterdam, The Netherlands, 2017.

[29] Y.G. Chen, X.M. Guo, Dynamic defrosting characteristics of air source heat pump and effects of outdoor air parameters on defrost cycle performance, Applied Thermal Engineering 29 (2009) 2701-2707.